

CIRCUIT DESIGN FOR A MEASUREMENT-BASED QUANTUM CARRY-LOOKAHEAD ADDER

AGUNG TRISETYARSO^a

*Department of Applied Physics and Physico-Informatics, Keio University,
3-14-1 Hiyoshi, Kohoku-ku, Yokohama-shi, Kanagawa-ken 223-8522, Japan*

RODNEY VAN METER^b

*Faculty of Environment and Information Studies, Keio University,
5322 Endo, Fujisawa-shi, Kanagawa-ken 252-8520, Japan*

Received (received date)

Revised (revised date)

We present the design and evaluation of a quantum carry-lookahead adder (QCLA) using measurement-based quantum computation (MBQC), called MBQCLA. MBQCLA utilizes MBQC's ability to transfer quantum states in unit time to accelerate addition. The quantum carry-lookahead adder is faster than a quantum ripple-carry adder; QCLA has logarithmic depth while ripple adders have linear depth. MBQCLA is an order of magnitude faster than a ripple-carry adder when adding registers longer than 100 qubits, but requires a cluster state that is an order of magnitude larger. The cluster state resources can be classified as computation and communication; for the unoptimized form, $\approx 88\%$ of the resources are used for communication. Hand optimization of horizontal communication costs results in a $\approx 12\%$ reduction in spatial resources for the in-place MBQCLA circuit.

Keywords: Quantum Carry-Lookahead Adder, Cluster-State Computation

Communicated by: to be filled by the Editorial

1 Introduction

Measurement-based quantum computation (MBQC) is a new paradigm for implementing quantum algorithms using a quantum cluster state [1][2][3][4]. A cluster state is a highly entangled state of qubits which can serve as the resource for universal quantum computation. By subsequent single-qubit measurements, quantum gates are effected on the logical qubits encoded in the cluster state. Quantum information propagation in a cluster is driven by the pattern of measurement bases, regardless of the measurement outcomes. MBQC is attractive because cluster states are considered to be easy to create on systems ranging from the polarization state of photons [5] to Josephson junction qubits [6].

A cluster state can be built on a two-dimensional rectangular lattice with Manhattan geometry. Some of the qubits in the cluster state are data qubits, while the rest are created in a generic entangled state. Employing quantum correlations for quantum computation, as

^atrisetyarso07@a8.keio.jp

^brdv@sfc.wide.ad.jp

stated in Raussendorf’s first theorem in [4], quantum gates on the data qubits can be evaluated by measuring lattice qubits in a particular basis. All gates in the Clifford group, including CNOT, can be performed in one time step via a large number of concurrent measurements. Remarkably, because both wires and SWAP gates are in the Clifford group, MBQC supports long-distance gates in a single time step even when the cluster state is built on a physical system permitting only nearest-neighbor interactions. The Toffoli Phase gate can be executed in two time steps, where the measurement basis for the second step is selected depending on previous measurement outcomes. This adaptive process determines the overall performance of many algorithms.

Thus, a cluster state can be used to execute arbitrary quantum algorithms. MBQC algorithms are often created by mapping known quantum circuits onto the cluster state. The challenge is to find application algorithms that match the strengths of MBQC. Here, we choose to address the problem of integer addition.

Addition is a critical subroutine for algorithms such as Shor’s algorithm for factoring large numbers [7][8][9][10]. Addition can be executed in many ways, with its performance being primarily dependent on carry propagation, which is normally limited by the physical architecture[11][12]. The simplest method is ripple-carry addition, which has depth of $O(n)$ [8][9][13][14]. In a ripple-carry adder, carry information is propagated from the low-order qubits to the high order qubits one step at a time.

The goal of our work is to reduce the execution time of addition on MBQC. Raussendorf et al. successfully mapped the VBE ripple-carry adder to MBQC bending the circuit layout to reduce the spatial resources[4][8]. However, a ripple-carry adder does not take good advantage of the strengths of MBQC. By unifying the Quantum Carry-Lookahead Adder (QCLA)[15] with MBQC, we have designed a much faster circuit. In this paper, we present our design for the MBQCLA and evaluate the design in terms of its execution speed and resource requirements.

The paper is organized as follows: the basic notions of Measurement-Based Quantum Computation and Quantum Carry-Lookahead Adder are given in Section 2. Section 3 contains the implementation of MBQC form for QCLA circuits. Here, the out-of-place, in-place, and the optimized version of in-place circuits are discussed to obtain their performances and requirements. We conclude in Section 4. Appendix A gives a detailed exposition of a NOT gate in cluster state and the graphical notation used in this paper. Appendix B contains the procedures to implement the out-of-place and in-place QCLAs in abstract quantum circuit form. Appendix C provides the requirements and performance for MBQCLA circuits.

2 Background

Our proposal is built based on two concepts:(a) Measurement-Based Quantum Computation, and (b) the Quantum Carry-Lookahead Adder. In this section, we will present a short review of these concepts.

2.1 Measurement-Based Quantum Computation

A one-dimensional cluster state is in the form of

$$|\Phi_N\rangle = \frac{1}{2^N} \bigotimes_{a=1}^N \left(|0\rangle_a \sigma_v^{(a+1)} + |1\rangle_a \right), \quad (1)$$

where $\sigma_v^{(i)}$ is the Pauli operator operating on qubit i in the N -qubit cluster \mathcal{C} , a is the index of a qubit in cluster \mathcal{C} and v can be x, y , or z depending on the choice of interaction Hamiltonian between neighbors[5] and with the convention $\sigma_v^{N+1} = 1$. In general, the cluster state should obey the quantum correlation equation

$$\bigotimes_{a,v} \sigma_v^{(a)} \left| \Phi_{\{k\}} \right\rangle_{\mathcal{C}} = (-1)^{k_a} \left| \Phi_{\{k\}} \right\rangle_{\mathcal{C}}, \quad (2)$$

where $v=I, x, y, z$, and $k_a = \{0, 1\}$. The parameter $\{k\}$ is a set of index parameters specifying the cluster state. $\left| \Phi_{\{k\}} \right\rangle_{\mathcal{C}}$ expresses the cluster state before the measurement and $\left| \Psi_{\{k\}} \right\rangle_{\mathcal{C}(g)}$ represents the cluster state after a set of measurements in which quantum gate g has been simulated on the cluster state. The cluster state can be created in several ways, e.g., initializing every qubit to the $|+\rangle$ state and performing a Controlled- Z gate between each neighboring pair. The main notion of measurement-based quantum computation is the first theorem of Raussendorf et al. [4]. Any quantum computation can be obtained by certain measurement patterns.

Suppose we have an initial set of cluster state eigenvalue equations, $\left| \Phi_{\{k\}} \right\rangle_{\mathcal{C}}$, representing the cluster which is the union of the input cluster (\mathcal{C}_{input}), the machine cluster, ($\mathcal{C}_{machine}$) and the output cluster (\mathcal{C}_{output}) with there are no intersection between each other, then it is measured by the projective measurement operators \mathcal{P} with certain measurement patterns \mathcal{M} , $\mathcal{P}_{\{s\}}^{(C)}(\mathcal{M}) = \bigotimes_{k \in \mathcal{C}} \frac{1 + (-1)^{k_a} \vec{r}_k \cdot \vec{\sigma}^{(k)}}{2}$. The measurement outcome is the cluster state $\left| \Psi_{\{k\}} \right\rangle_{\mathcal{C}(g)}$ obeying $2n$ eigenvalue equations:

$$\sigma_x^{(\mathcal{C}_{input(g),i})} (U \sigma_x^{(i)} U^\dagger)^{(\mathcal{C}_{output(g)})} |\psi\rangle_{\mathcal{C}(g)} = (-1)^{\lambda_{x,i}} |\psi\rangle_{\mathcal{C}(g)} \quad (3)$$

$$\sigma_x^{(\mathcal{C}_{input(g),i})} (U \sigma_x^{(i)} U^\dagger)^{(\mathcal{C}_{output(g)})} |\psi\rangle_{\mathcal{C}(g)} = (-1)^{\lambda_{z,i}} |\psi\rangle_{\mathcal{C}(g)}, \quad (4)$$

where $\lambda_{x,i}, \lambda_{z,i} \in \{0, 1\}$ are the measurement outcomes.

The *Theorem* shows quantum computation in Clifford algebra form implicitly appears in the final set of eigenvalue equations after the measurements. A detailed explanation is given in Appendix A.

Several remarkable properties follow from this *Theorem*[2][16]:

- Measurement of qubits in the machine cluster in the σ_z -eigenbasis removes them from the main cluster and **disconnects** all of the their bonds.
- Measurement of qubits in the machine cluster in the σ_x -eigenbasis removes them from the main cluster and creates **Bell pairs** between the qubits in input cluster and the qubits in the output cluster.
- Measurement of qubits in the machine cluster in the σ_y -eigenbasis removes them from the main cluster and leaves an entangled state between the qubits in the input cluster and the qubits in the output cluster.

The physical implementation of MBQC requires a lattice system with an Ising-like interaction between the qubits so that the quantum information can be propagated in the lattice due to the measurement. Several physical implementations have been proposed; Meier et al.

proposed the possibility of experimental realization to perform initialization, quantum gate operation and read-out mechanism in antiferromagnetic spin cluster quantum computing[17]. Devitt et al. have described an all-optical implementation where the required number of photonic modules and chips only depends on the cross section length of the two-dimensional lattice (corresponding to the y -axis in our figures)[18][19].

MBQC runs in two phases: prepare the cluster state, then measure. Because the preparation step is completely generic, failure in coupling the qubits is not a problem. Mechanisms that succeed only probabilistically can be used, as long as failures are heralded, making optical QC suitable for MBQC.

2.2 *Quantum Carry-Lookahead Adder*

The Quantum Carry-Lookahead Adder (QCLA) was designed by Draper et al.[15]. The quantum carry-lookahead adder is potentially more efficient than a quantum ripple-carry adder since its depth is $O(\log n)$. A carry-lookahead adder uses three phases, the ‘‘Generate’’ (G), ‘‘Propagate’’ (P), and ‘‘Kill’’ (K) networks, each of which progressively doubles the length of its span in each time step, to calculate the complete ‘‘Carry’’ values (C). In practice, the networks are somewhat redundant, and Draper et al. defined their circuit using only the P and G networks to calculate the final carry C. The out-of-place form of the QCLA performs the unitary transformation $|a, b, \theta\rangle \rightarrow |a, b, a + b\rangle$, and the in-place form calculates $|a, b\rangle \rightarrow |a, a + b\rangle$ where $|a\rangle, |b\rangle$ and $|a + b\rangle$ are n -qubit registers, where θ is the low-order qubit and $n-1$ is the high-order qubit.

The carry-lookahead adder starts with an initial addition round, consisting of a half adder for each qubit in the logical register. Starting from the basic idea of the carry-lookahead adder originally designed for classical binary logic[20], the carry is propagated from bit to bit $i \rightarrow j \rightarrow k$, where $i \leq j \leq k$, so carry equations or majority blocks are represented by:

$$c_j = g[i, j] \oplus p[i, j] \wedge c_i \quad (5)$$

$$c_k = g[j, k] \oplus p[j, k] \wedge c_j \quad (6)$$

By straightforward substitution of these equations, we have the equation:

$$c_k = g[j, k] \oplus p[j, k] \wedge (g[i, j] \oplus p[i, j] \wedge c_i) \quad (7)$$

or

$$c_k = g[j, k] \oplus p[j, k] \wedge g[i, j] \oplus p[i, j] \wedge p[j, k] \wedge c_i \quad (8)$$

Substituting by $c_k = g[i, k] \oplus p[i, k] \wedge c_i$ into Eq.(8) gives:

$$g[i, k] = g[j, k] \oplus p[j, k] \wedge g[i, j]. \quad (9)$$

A circuit that performs this computation in a lookahead adder is called the Generate network. Similarly, a circuit that implements the equations

$$p[i, k] = p[i, j] \wedge p[j, k] \quad (10)$$

for any $i < j < k$ is called the Propagate network. The implementation of these networks in reversible computation is realized by the following steps where n is logical qubits, t is the round number and m is the index of qubits in the register:

1. *P*-rounds. For $t=1$ to $\lfloor \log n \rfloor - 1$: for $1 \leq m < \lfloor n/2^t \rfloor$. Then the connection between the steps in this round is expressed by: $P_t[m] \oplus = P_{t-1}[2m] P_{t-1}[2m+1]$.
2. *G*-rounds. For $t=1$ to $\lfloor \log n \rfloor$: for $0 \leq m < \lfloor n/2^t \rfloor$. And, the relation between the steps in the round is: $G[2^t m + 2^t] \oplus = G[2^t m + 2^{t-1}] P_{t-1}[2m+1]$.
3. *C*-rounds. For $t = \lfloor \log 2n/3 \rfloor$ down to 1: for $1 \leq m < \lfloor (n-2^{t-1})/2^t \rfloor$. The connection between the steps in the round is represented by: $G[2^t m + 2^{t-1}] \oplus = G[2^t m] P_{t-1}[2m]$.

These networks will be applied both to out-of-place and in-place QCLA circuits. Those circuits, which are distinguished by the form of the addition scheme, are explained in more detail in Appendix B.

3 Quantum Carry-Lookahead Adder for Measurement-Based Quantum Computation

This section explains the implementation of QCLA for MBQC. The performance and requirements for both out-of-place and in-place MBQCLA circuits schemes are evaluated. First we describe our metrics for evaluating circuits. The exposition of direct mapping on both schemes is given, followed by the optimization for the in-place circuit. The optimization is done by adjusting the border between the rounds of the circuit, then removing the unnecessary lattice sites between the quantum gates, reducing the communication costs in the circuit. More detailed results are presented in Appendix C.

3.1 Evaluating Algorithms Executed using MBQC

Logical quantum circuits can be evaluated based on the execution time or circuit depth (usually measured in numbers of Toffoli gates), number of qubits used, and total number of gates executed. The number of logical qubits is the number of required input qubits plus the number of ancillae required in the circuit representation of the algorithm.

We propose the use of (a) execution time, (b) circuit area, (c) number of qubits in the cluster state, and (d) the number of clustering operations necessary to make the state as measures of performance and cost for algorithms executed using MBQC. The number of cluster operations is specified as the number of successful interactions needed. The circuit area is the height of the cluster times its width, assuming a regular rectangular lattice. All of these measures can be expressed in terms of problem size; in our case, in terms of n , the length of each of the logical registers being added.

The goal of this paper is to minimize the execution time, while the other three are measures of the cost. These costs, as shown in Figure 1, can be divided into two categories: *first, computational resources*, i.e., the number of cluster qubits required for Toffoli Phase, CNOT and NOT gates. *Second, communication resources*, i.e., the number of cluster qubits required for SWAP gates and wires. A circuit which uses no communication resources is called an **optimal circuit**. As noted above, MBQC requires a measure-adapt-measure cycle to implement non-Clifford gates. The execution time is the number of rounds of measurement, followed by computation of the adaptive bases for the next round.

In general, the optimal circuit resources can be determined summing the resources con-

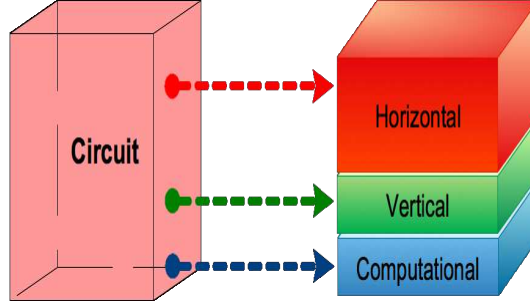


Fig. 1. Illustration for circuit costs for MBQCLA. The costs contain computational and communication costs. The resources for communication costs can be separated into two types of resources: horizontal (wires) and vertical (SWAP gates).

sumed by the various types of computational gates. Thus, it is expressed by

$$\sum_{i \in \text{Quantum Gate}} \mathcal{X}_i \mathcal{R}_i \quad (11)$$

where

- \mathcal{X}_i = Number of quantum gate- i
- \mathcal{R}_i = Qubit resources for quantum gate- i

Because the QCLA is structured in a set of rounds, each of which contains only gates of a single type (e.g. Toffoli Phase Gate), we can discuss the cost in those terms. The cost of a null circuit would simply be the number of logical qubits multiplied by the cost of a horizontal wire. In an actual circuit, we replace some sections of horizontal wire with logical gates, and add vertical wires with SWAP gates as necessary to implement the logic. Thus, each round in the QCLA, when mapped onto the cluster state, is as wide as necessary to accommodate the necessary gate type.

By considering the number of SWAP, Toffoli and CNOT gates in the initial addition circuit and in P,G and C networks as shown above, we can approximate the physical resources needed for the out-of-place MBQCLA following this expression:

$$\text{Size} \approx \sum_i (\mathcal{V}(n) \times \mathcal{B}_i \times \mathcal{T}_i + \mathcal{X}_i (\mathcal{R}_i - \mathcal{E}_i \times \mathcal{T}_i)) + \mathcal{L}_{SWAP} \times \mathcal{S}_{SWAP} \quad (12)$$

where $i \in \{\text{Toffoli Phase, CNOT, and NOT Gates}\}$, $\mathcal{V}(n)$ = number of logical qubits, \mathcal{B}_i = number of rounds for the gate of type i , \mathcal{X}_i = number of gates of type i , \mathcal{T}_i = width of the i -gate (in lattice sites), \mathcal{R}_i = number of lattice qubits in an i -gate, \mathcal{E}_i = number of logical qubits in an i -gate (generally, one to three), \mathcal{L}_{SWAP} is number of lattice qubits in a cluster state SWAP gate and \mathcal{S}_{SWAP} = number of SWAP gates in a QCLA circuit which is dependent on the mapping of the logical qubits to positions on the lattice.

In Equation (12), $\sum_i (\mathcal{V}(n) \times \mathcal{B}_i \times \mathcal{T}_i)$ is the cost of a lattice large enough to hold all of the circuit rounds that use type i -gates (that is horizontal communication costs). $-\sum_i \mathcal{E}_i \times \mathcal{X}_i \times \mathcal{T}_i$ is adjustment for replacing wires with logic gates. $\mathcal{L}_{SWAP} \times \mathcal{S}_{SWAP}$, which depends on type

of rounds in QCLA circuit, is the vertical communication in the circuit, which is entirely SWAP gates resources.

Proposed implementations of cluster state quantum computing in solid-state technologies, which need Ising-like Hamiltonian[6][21] [22][23][17], operate on a fixed 2-D lattice. Hence, they require wires for communication between the rounds, which means those proposals will use our optimized circuit. A photonic-based quantum computer[19][18] will require no wires for communication between the rounds, allowing the optimal circuits to be used more or less directly.

3.2 *Out-of-place Measurement-Based Quantum Carry-Lookahead Adder*

Our design for a 10-bit form of the out-of-place QCLA on MBQC is shown in Figure 2. The input qubits are on the left (top in the rotated figure) and output states are on the right. In the figures in this paper, a pink square qubit represents a cluster qubit measured in the σ_x -eigenbasis measurement, a green qubit is for π -rotation on σ_x -eigenbasis measurement, a red qubit is for σ_y -eigenbasis measurement and a blue qubit is for σ_z -eigenbasis measurement. The propagation pattern of one logical qubit is highlighted in yellow. Our logical qubits are spaced with a pitch of four lattice sites to accommodate the necessary spacing between gates. Each large box outlines one round in the P, G or C networks. The circuit is presented in unoptimized form for clarity.

This circuit is essentially a direct mapping of the abstract out-of-place QCLA (Figure B.1) to MBQC. The logical gates used are those described in Figure A.2. As noted above, in addition to the computational resources, we must add wires and SWAP gates. The long distance gates from the abstract out-of-place QCLA (Figure B.1) are executed using the scheme for non-adjacent computation (Figure A.3). To completely characterize the circuit, we need to know how many SWAP gates and wire segments are added to complete the circuit. The exact cost depends on the layout of logical qubits. Below we calculate the number of SWAP gates required assuming the data layout of Figure 2.

The abstract circuit consists of addition and carry computation circuits. The addition circuit, which has depth 4, is built from n Toffoli gates and $3n-1$ CNOT gates while the carry computation machinery consists of $4n-3w(n)-3\lfloor \log n \rfloor -1$ Toffoli gates and its depth is $\lfloor \log_2(n) \rfloor + \lfloor \log_2(n/3) \rfloor + 3$. The number of Toffoli gates in this circuit can be obtained by adding the number of Toffolis in the addition, P, G, and C networks. For the out-of-place QCLA circuit, we have $n-w(n)-\lfloor \log n \rfloor$ Toffoli gates for the P network, $n-w(n)$ Toffoli gates for the G network and $n-\lfloor \log n \rfloor -1$ for C network, where $w(n)$ is the Hamming weight of the binary representation of n . Furthermore, the number of SWAP gates, which is the vertical communication resources, can be obtained as follows:

- The initial addition round needs

$$\mathcal{S}_{Ad} = 4n - 2w(n) - 2\lfloor \log_2(n) \rfloor \quad (13)$$

SWAP gates. For $n=10$, we need 30 SWAP gates consuming 360 lattice qubits.

- The propagate network needs 28 SWAP gates for $n=10$. This number can be obtained from the number of Toffoli gates for each round, $\lfloor n/2^{t_p} \rfloor -1$ where t_p is the round number in the propagate network, $1 \leq t_p \leq \lfloor \log_2 n \rfloor -1$. There are 4 Toffoli gates in first P-round

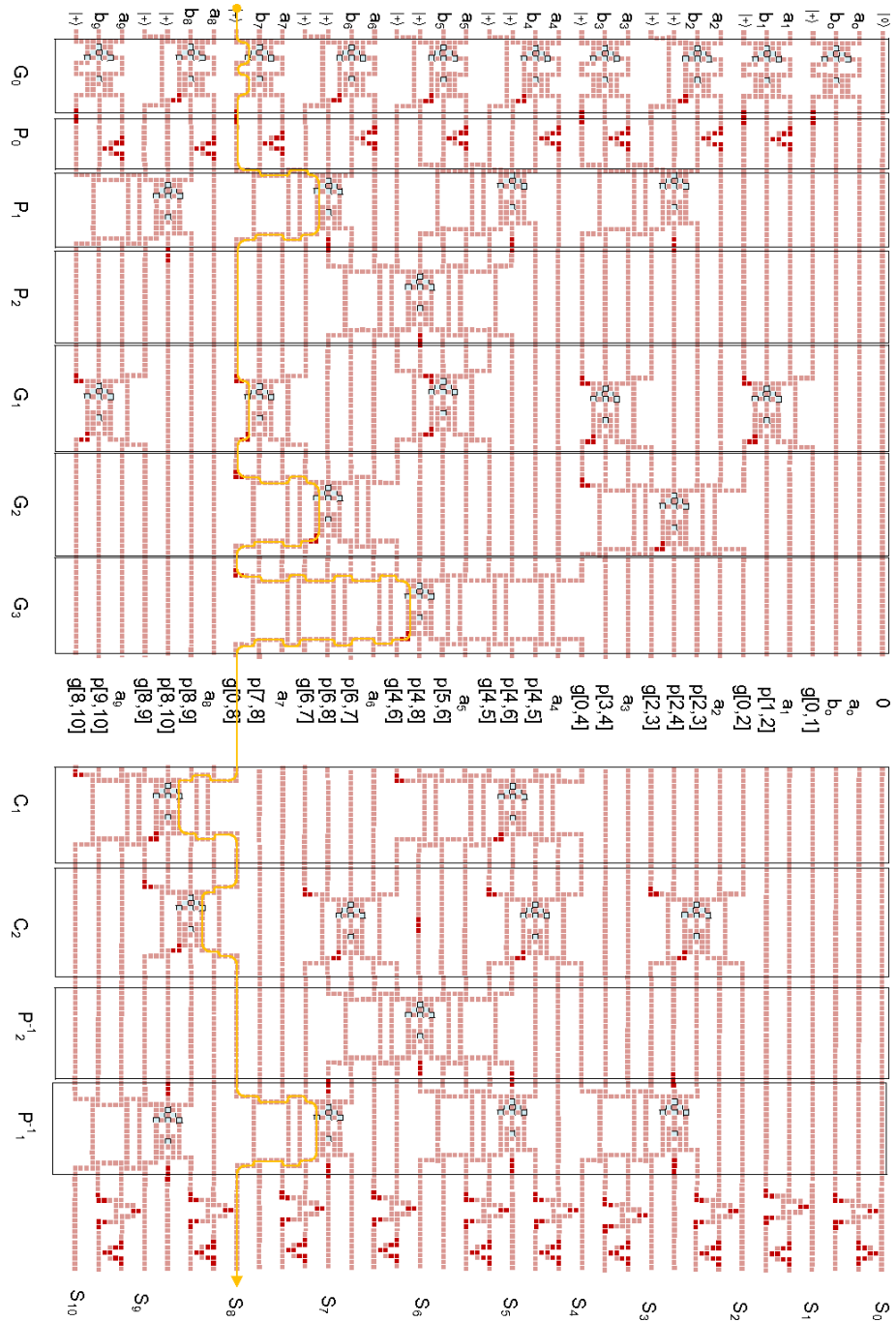


Fig. 2. Out-of-place MBQCLA. For $n=10$, the circuit consists of: 4 addition blocks, 9 rounds of gates for the carry networks (2 Propagate, 3 Generate, 2 Inverse Propagate and 2 Carry networks). For explanation of the colors, see Appendix A.

with 16 SWAP gates and 1 Toffoli gate in second P-round with 12 SWAP gates. The equation representing vertical communication in P networks is

$$\mathcal{S}_P = \sum_{t_p=1}^{\log_2(n)-1} 2n - 2^{t_p+1} \quad (14)$$

- Similarly, the generate network requires 58 SWAP gates for $n=10$. The number of Toffoli gates for each round is expressed by $5n+w(n)+2\lceil\log n\rceil$. As formulated by $\lfloor n/2^{t_g} \rfloor$, we have three rounds of generate networks; the first round consists of 5 Toffoli gates with 12 SWAP gates, the second round needs 2 Toffoli gates with 20 SWAP gates and the third round requires 1 Toffoli gate with 26 SWAP gates. The SWAP gates resources in G network can be approximated by

$$\mathcal{S}_G = \sum_{t_g=1}^{\log_2(n)} 4\lceil\log_2(n)\rceil + 2^{t_g+1}\lceil\log_2(t_g)\rceil \quad (15)$$

where t_g is the round in G network.

- The mathematical expression for the number of Toffoli gates in the carry network is $\lfloor n-2^{t_c-1}/2^{t_c} \rfloor$. Therein, the first Carry round has 4 Toffoli gates with 16 SWAP gates and its second round has 22 SWAP gates. Resources of SWAP gates in C network can be obtained by

$$\mathcal{S}_C = \sum_{t_c=1}^{\lfloor\log_2 \frac{2n}{3}\rfloor} 2n - 2\lceil\log_2(t_c)\rceil \quad (16)$$

where t_c is the round in C network.

Following the Equation (12), \mathcal{S}_{SWAP} is the sum of Equations (13), (14), (15), and (16)

$$\mathcal{S}_{SWAP} = \mathcal{S}_{Ad} + \mathcal{S}_P + \mathcal{S}_G + \mathcal{S}_C \quad (17)$$

For the out-of-place MBQCLA, we see that the depth is reduced to $\lceil\log_2(n)\rceil + \lceil\log_2(n/3)\rceil + 7$ compared to $\approx 3n$ for the VBE ripple-carry. However, this circuit costs more in physical resources, $\approx 901n + 224n \times \lceil\log_2(n)\rceil$ compared to $\approx 304n$ for the VBE ripple-carry. The comparison of size and depth between MBQC VBE and MBQCLA is shown in Figure 3.

3.3 In-place Measurement-Based Quantum Carry-Lookahead Adder

The next step is obtaining the performance and requirements of the in-place quantum carry look-ahead adder. Following the scheme in [15], the erasure (uncomputation) of the low-order $n-1$ bits of the carry string c requires additional circuitry. The algorithm for in-place is more complex than out-of-place and uses about twice as many Toffoli gates.

The subsequent procedures, as provided in the Appendix B, give in-place MBQCLA circuit horizontal resources (Table C.2). The abstract in-place QCLA has the overall depth $\lceil\log n\rceil + \lceil\log(n-1)\rceil + \lceil\log \frac{n}{3}\rceil + \lceil\log \frac{n-1}{3}\rceil + 14$ which is also the depth for its in-place MBQC form, counted in terms of measurement operations rather than Toffoli gate times.

As shown in the previous section, the vertical communication resources can be estimated by counting the number of SWAP gates in the circuit. There are $6n-4w(n)-4\lceil\log n\rceil-2$ SWAP

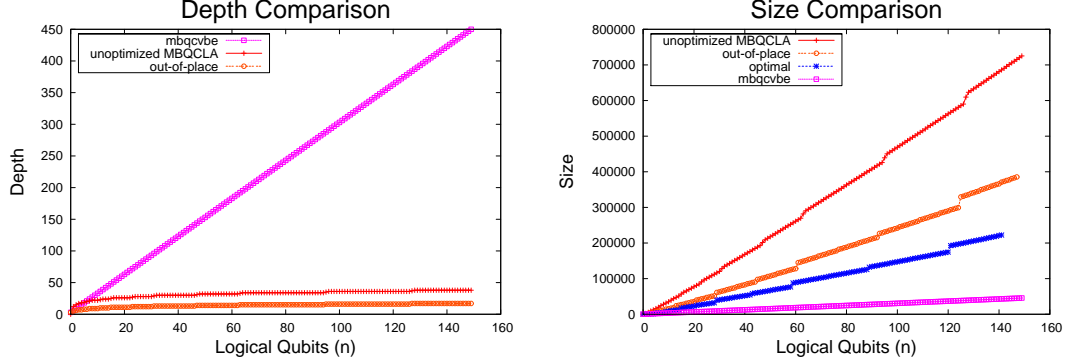


Fig. 3. Size and depth comparison between MBQC VBE and MBQCLA. “+”, “*”, “o” and “□” marks are for in-place, optimized in-place, out-of-place and MBQC VBE circuits, respectively.

gates to provide ancilla register needed for addition in-place MBQCLA circuit. The other SWAP gate resources can be obtained by examining the Propagate, Generate, and Carry networks. In the in-place circuit we need sequences both circuits for computing and uncomputing the carry status meaning $8n+14\lfloor\log n\rfloor+2$ SWAP gates are needed for non-adjacent quantum computation. Straightforward derivation of Equation(12), physical resources for in-place circuit is

$$\approx 2896n + 64n\lfloor\log_2(n)\rfloor \quad (18)$$

Also, by the use of Equations (13)(14)(15) and (16) for out-of place circuit, the vertical communication resources (SWAP gates, especially), or \mathcal{S}_{SWAP} for in-place MBQCLA circuit can be determined as follow

$$\mathcal{S}_{SWAP} = \mathcal{S}_{Ad} + \mathcal{S}'_{Ad} + 4\mathcal{S}_P + 2\mathcal{S}_G + 2\mathcal{S}_C \quad (19)$$

where $\mathcal{S}'_{Ad} = \sum_{i=1}^n 2(n-1)$, is an additional column required to perform an in-place circuit.

It is also useful to obtain the mathematical expression of optimal in-place MBQCLA circuit. According to Equation [11], the equation is given by

$$= \mathcal{X}_{TPG}\mathcal{R}_{TPG} + \mathcal{X}_{CNOT}\mathcal{R}_{CNOT} + \mathcal{X}_{NOT}\mathcal{R}_{NOT} \quad (20)$$

By the use of Table [B.1], one can obtain

$$162(w(n) + \lfloor\log_2(n-1)\rfloor + \lfloor\log_2(n)\rfloor - w(n-1)) + 542n - 395 \quad (21)$$

3.4 Optimized In-place MBQCLA

In this section, we present the design of an optimized form of the in-place MBQCLA. The idea of the bent network[4], imagining that logical qubits are propagated through pipes on a two-dimensional surface, is used to reduce the horizontal resources of MBQCLA.

3.4.1 Bent Network in Quantum Carry-Lookahead Adder

Contrary to the usual quantum circuit assumption that the horizontal axis relates to logical time, in a "bent" network the temporal axis flows freely in the spatial layout. The consequence is that a more compact circuit can be constructed.

If we apply this bent network method to MBQCLA, we also find that we can reduce the horizontal size of the circuit. The bent form of VBE is purely rectangular, but MBQCLA is not as regular. The horizontal size for every logical qubit position will depend on the number of quantum gates, since it will vary along the register as shown in Fig.6. The illustration of a bent network implementation for $n=10$ is given in Fig.7.

3.4.2 Optimized Circuit Formulation

To optimize the circuit, we take small groups of qubits, or subregisters, and slide them toward the middle of the circuit. As can be seen in Fig.7, bending the network can reduce the cluster resources required near qubits $a_0, a_1, a_2, a_3, a_4, a_6, a_8,$ and a_9 by the amount:

$$\sum_{i=0}^{n-1} (\mathcal{C}_i \mathcal{A}_i \mathcal{W}) \quad (22)$$

where n = number of logical qubits, \mathcal{C}_i = the number of rounds (columns) that i th-subregister moves, \mathcal{A}_i = number of logical qubits in the i th-subregister (usually 3, sometimes 4), and \mathcal{W} = width of Toffoli Phase Gate. For $n=10$, this manual optimization of horizontal communication results in a reduction of $\approx 12\%$ for spatial resources, or ≈ 3822 qubits.

According to Equations (19), (21), and (18), the quantitative explanation of MBQCLA resources is provided in Figure 4. The red area, which represents the horizontal communication costs of MBQCLA, is $\approx 77\%$ of the qubits in the cluster. The light green area, showing the costs of MBQCLA circuit vertical communication, consumes $\approx 11\%$. The cost of the computational circuit shown by the light blue area is $\approx 12\%$ of the spatial resources.

4 Conclusion

In this work, the circuit designs for a Measurement-Based Quantum Carry-Lookahead Adder (MBQCLA) are presented. We have shown the resources required to perform the quantum carry-lookahead adder in cluster state as a function of the number of logical qubits, width of quantum gates, and number of qubits in quantum gates. By bending the network and removing the border between the rounds, the optimization of the in-place MBQCLA circuit changes its shape from Manhattan grid to diamond-like form. The proposed evaluation methods for the cost and performance of application circuits for MBQC will be useful for large scale quantum computer architecture, since application circuits for quantum computers will need optimization similar to that done for classical computer technology. This work has shown the value of finding application algorithms that match the strengths of measurement-based quantum computation.

Acknowledgments We would like to thank Seth Lloyd, Kohei M. Itoh, Austin Fowler, and Achmad Husni Thamrin for fruitful discussions. This work was supported in part by Grant-in-Aid for Scientific Research by MEXT, Specially Promoted Research No. 18001002 and in part by Special Coordination Funds for Promoting Science and Technology.

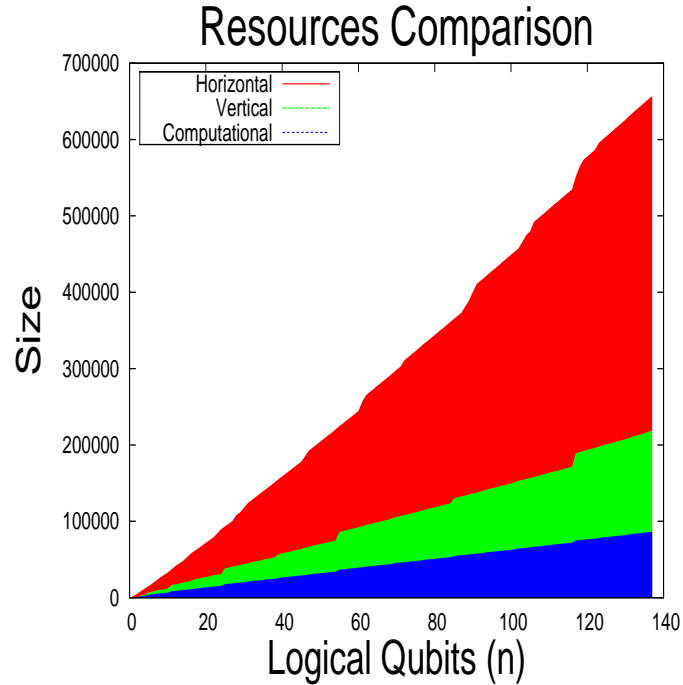


Fig. 4. Comparison of computational and communication resources in in-place MBQCLA circuit. The bottom line on the graph represents the ideal circumstance for the computational resource and the other two show the circuit with additional resources for the horizontal and the vertical communications.

1. H. J. Briegel, D. E. Browne, W. Dur, R. Raussendorf, and M. Van den Nest, *Nature Physics*, 19 (2009).
2. R. Raussendorf and H. J. Briegel, *Phys. Rev. Lett.* **86**, 5188 (2001 May 28).
3. H. J. Briegel and R. Raussendorf, *Phys. Rev. Lett.* **86**, 910 (2001 Jan 29).
4. R. Raussendorf, D. E. Browne, and H. J. Briegel, *Phys. Rev. A* **68**, 022312 (2003).
5. P. Walther *et al.*, *Nature* **434**, 169 (2005 Mar 10).
6. T. Tanamoto, Y.-x. Liu, S. Fujita, X. Hu, and F. Nori, *Phys. Rev. Lett.* **97**, 230501 (2006 Dec 8).
7. P. W. Shor, *SIAM J. Comput.* **26**, 1484 (1997).
8. V. Vedral, A. Barenco, and A. Ekert, *Phys. Rev. A* **54**, 147 (1996 Jul).
9. D. Beckman, A. Chari, S. Devabhaktuni, and J. Preskill, *Phys. Rev. A* **54**, 1034 (1996 Aug).
10. R. Van Meter and K. M. Itoh, *Phys. Rev. A* **71**, 052320 (2005).
11. R. Van Meter and M. Oskin, *ACM Journal on Emerging Technologies in Computing Systems* **2**, 31 (2006).
12. B.-S. Choi and R. Van Meter, Effects of interaction distance on quantum addition circuits, *quant-ph:0809.4317*, 2008.
13. S. A. Cuccaro, T. G. Draper, S. A. Kutin, and D. P. Moulton, A new quantum ripple-carry addition circuit, *arXiv:quant-ph/0410184v1*, 2004.
14. Y. Takahashi and N. Kunihiro, *Quantum Information & Computation* **5**, 440 (2005).
15. T. G. Draper, S. A. Kutin, E. M. Rains, and K. M. Svore, *Quantum Information & Computation* **6**, 351 (2006).
16. D. E. Browne and T. Rudolph, *Phys. Rev. Lett.* **95**, 010501 (2005 Jul 1).
17. F. Meier, J. Levy, and D. Loss, *Physical Review B* **68** (2003).

18. A. Politi, M. J. Cryan, J. G. Rarity, S. Yu, and J. L. O'Brien, *Science* **320**, 646 (2008).
19. S. J. Devitt *et al.*, Topological cluster state computation with photons, arXiv:0808.1782v1, 2008.
20. M. D. Ercegovac and T. Lang, *Digital Arithmetic* (Morgan-Kaufman, San Francisco, 2004).
21. J. Q. You, X.-b. Wang, T. Tanamoto, and F. Nori, *Physical Review A* **75** (2007).
22. Y. Weinstein, C. Hellberg, and J. Levy, *Phys. Rev. A* **72** (2005).
23. F. Meier, J. Levy, and D. Loss, *Phys. Rev. Lett.* **90**, 047901 (2003 Jan 31).
24. D. Leung, *International Journal of Quantum Information* **2**, 33 (2004).

Appendix A MBQC Gates and Graphical Notation

To illustrate MBQC, we detail the operation of the NOT gate, as shown in Figure A.1. The cluster contains 5 qubits where \mathcal{C}_{input} is qubit 1, $\mathcal{C}_{machine}$ are qubit 2, 3 and 4 and \mathcal{C}_{output} is qubit 5. We begin from the cluster state eigenvalue equations for 5 qubits:

$$\sigma_x^{(1)} \sigma_z^{(2)} |\phi\rangle_{\mathcal{C}(\mathbf{NOT})} = |\phi\rangle_{\mathcal{C}(\mathbf{NOT})} \quad (\text{A.1})$$

$$\sigma_z^{(1)} \sigma_x^{(2)} \sigma_z^{(3)} |\phi\rangle_{\mathcal{C}(\mathbf{NOT})} = |\phi\rangle_{\mathcal{C}(\mathbf{NOT})} \quad (\text{A.2})$$

$$\sigma_z^{(1)} \sigma_z^{(2)} \sigma_x^{(3)} \sigma_z^{(4)} |\phi\rangle_{\mathcal{C}(\mathbf{NOT})} = |\phi\rangle_{\mathcal{C}(\mathbf{NOT})} \quad (\text{A.3})$$

$$\sigma_z^{(3)} \sigma_x^{(4)} \sigma_z^{(5)} |\phi\rangle_{\mathcal{C}(\mathbf{NOT})} = |\phi\rangle_{\mathcal{C}(\mathbf{NOT})} \quad (\text{A.4})$$

$$\sigma_z^{(1)} \sigma_z^{(4)} \sigma_x^{(5)} |\phi\rangle_{\mathcal{C}(\mathbf{NOT})} = |\phi\rangle_{\mathcal{C}(\mathbf{NOT})} \quad (\text{A.5})$$

After obtaining the quantum correlation of the cluster state, two measurement steps are performed: *first*, the σ_x measurement on qubit 2 and qubit 4,

$$|\phi'\rangle_{\mathcal{C}(\mathbf{NOT})} = \mathcal{P}_{x,s_2}^{(2)} \mathcal{P}_{x,s_4}^{(4)} |\phi\rangle_{\mathcal{C}(\mathbf{NOT})} \quad (\text{A.6})$$

This first measurement converts the initial quantum correlation to the eigenvalue equations:

$$\sigma_x^{(1)} \sigma_x^{(3)} \sigma_x^{(5)} |\phi'\rangle_{\mathcal{C}(\mathbf{NOT})} = |\phi'\rangle_{\mathcal{C}(\mathbf{NOT})} \quad (\text{A.7})$$

$$\sigma_z^{(1)} \sigma_z^{(3)} |\phi'\rangle_{\mathcal{C}(\mathbf{NOT})} = (-1)^{s_2} |\phi'\rangle_{\mathcal{C}(\mathbf{NOT})} \quad (\text{A.8})$$

$$\sigma_z^{(3)} \sigma_z^{(5)} |\phi'\rangle_{\mathcal{C}(\mathbf{NOT})} = (-1)^{s_4} |\phi'\rangle_{\mathcal{C}(\mathbf{NOT})} \quad (\text{A.9})$$

Furthermore, the eigenbasis of $\vec{r}_{xy}((-1)^{s_2}(-\eta)) \cdot \vec{\sigma}$, where $\vec{r}_{xy} \cdot \vec{\sigma} = \cos(\eta) \sigma_x + \sin(\eta) \sigma_y$, is chosen as the measurement basis on qubit 3 to realize the operation **NOT** by measurement pattern $\mathcal{M}(\mathbf{NOT})$. Mathematically, it can be expressed by:

$$|\psi\rangle_{\mathcal{C}(\mathbf{NOT})} = \mathcal{P}_{xy(\eta)}^{(3)} |\phi'\rangle_{\mathcal{C}(\mathbf{NOT})}, \quad (\text{A.10})$$

where $\mathcal{P}_{xy(\eta)}^{(3)} = \frac{1+(-1)^{s_3} \vec{r}_k \cdot \vec{\sigma}^{(k)}}{2}$. This second measurement generates two eigenvalue equations from equation (A.7), (A.8) and (A.9), which obey *Theorem 1* of Raussendorf *et. al.*:

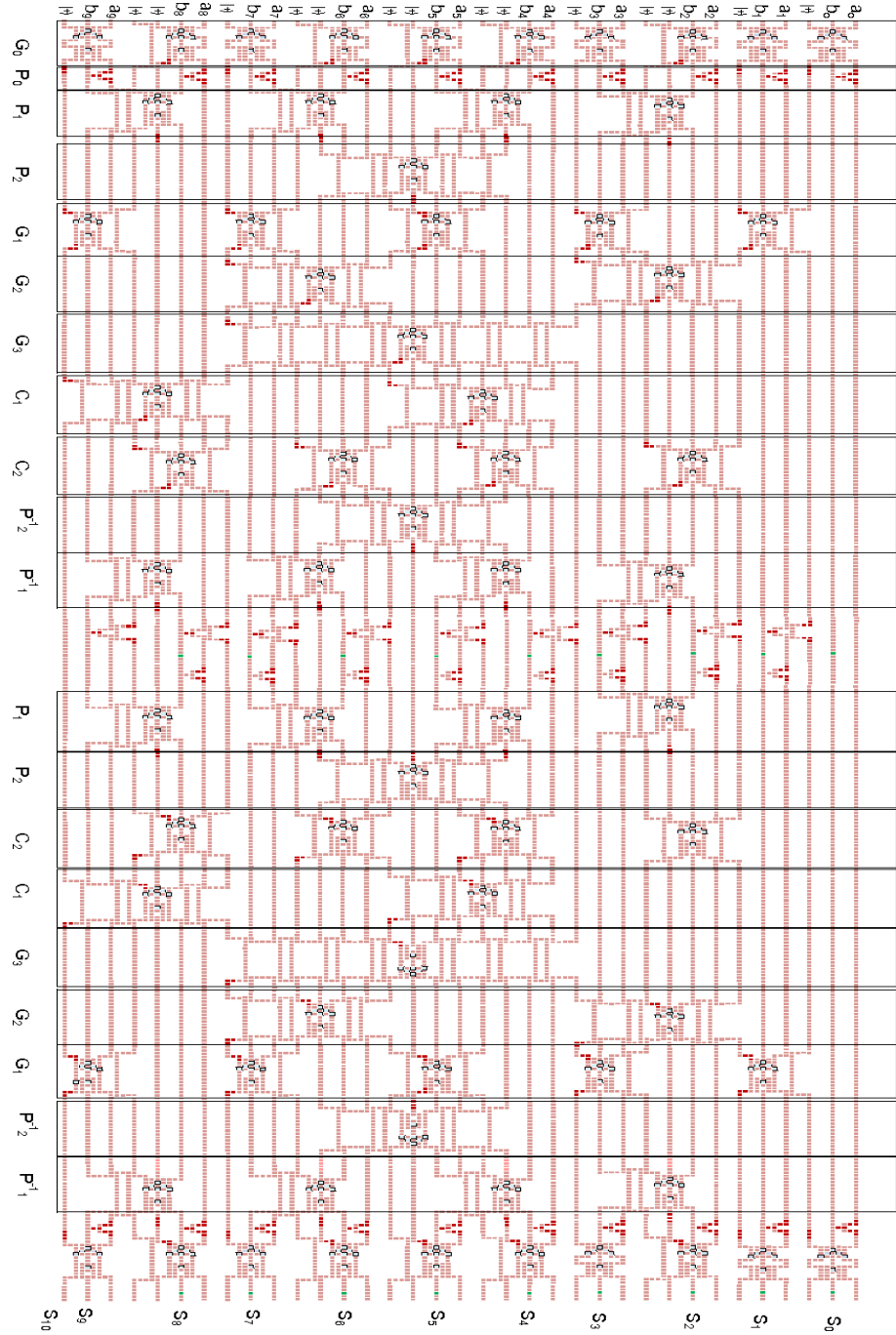


Fig. 5. In-place MBQCLA. For $n=10$, the circuit consists of:8 addition circuits, 18 carry networks (4 Propagate, 6 Generate, 4 Inverse Propagate and 4 Carry networks)

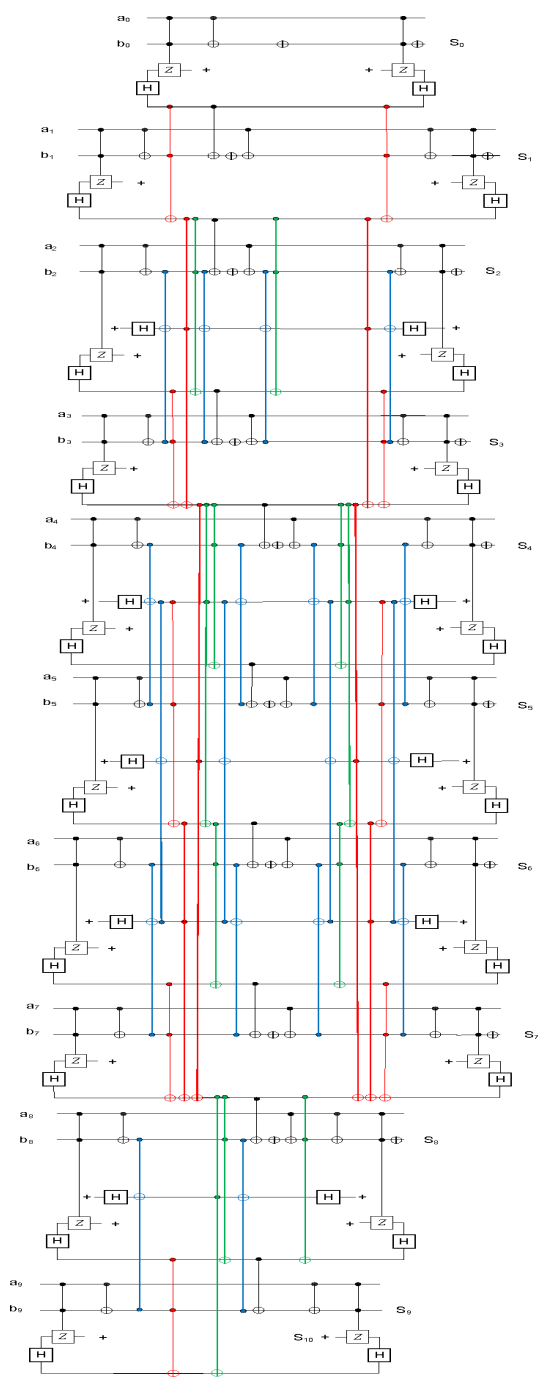


Fig. 6. Optimized in-place circuit. Low $n-1$ bits of the carry string output are tucked into the interior of the circuit by bending the network.

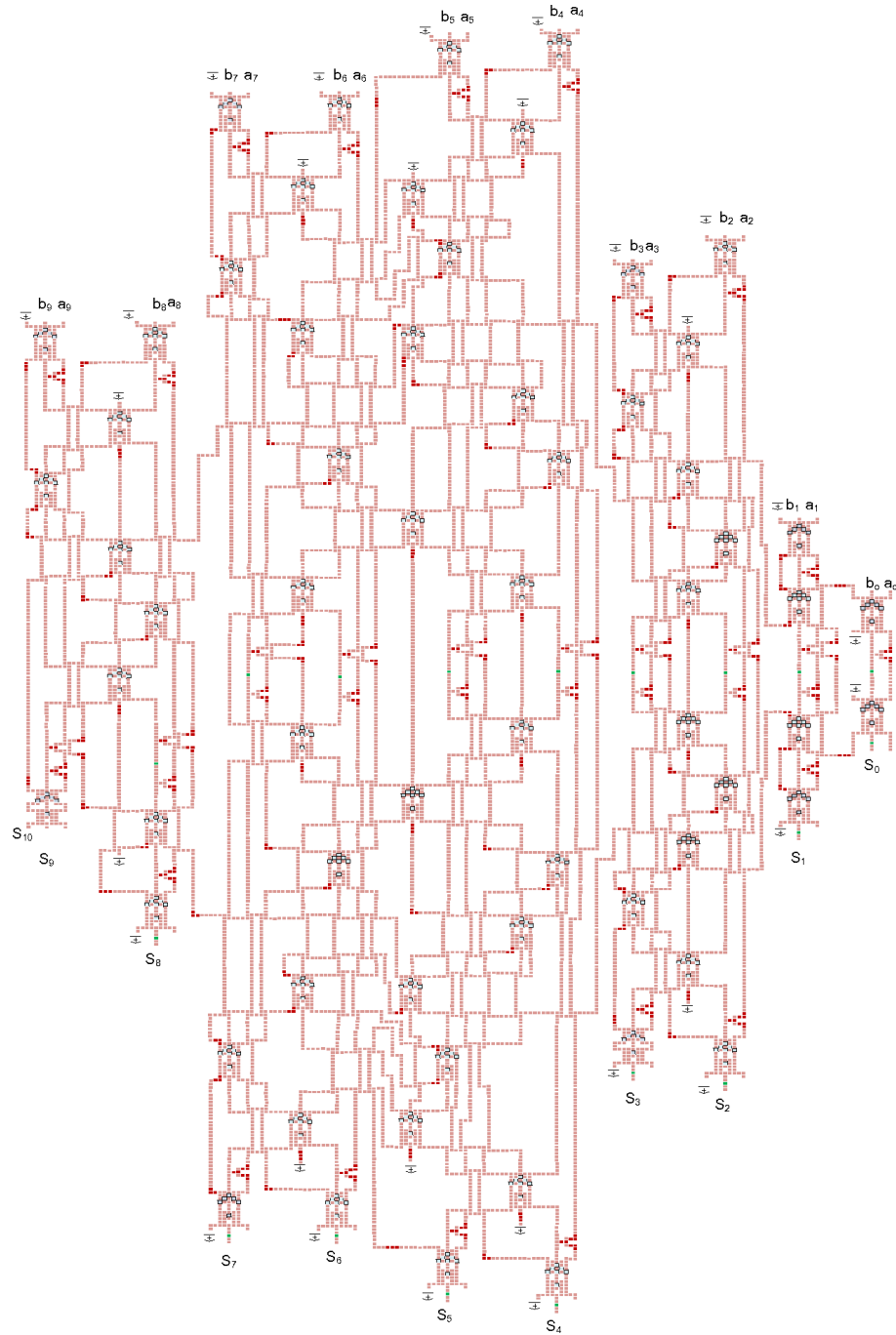


Fig. 7. Optimized in-place MBQCLA circuit corresponding to diamond-like form circuit, spatial resources optimization by hand is $\approx 12\%$ of horizontal communication.



Fig. A.1. NOT gate in MBQC. The input qubit and all pink qubits are measured in the σ_x -eigenbasis and the framed-green qubit is measured in an adaptive basis depending on the measurement outcome of qubit 2. Rotation measurement operator on xy -plane around z -axis with angle π on qubit 3 makes the qubit 3 not adaptive.

$$\sigma_x^{(1)} U^{(5)} [-\eta] \sigma_x^{(5)} U^{(5)\dagger} [\eta] |\psi\rangle_{C(\mathbf{NOT})} = |\psi\rangle_{C(\mathbf{NOT})} \quad (\text{A.11})$$

$$\sigma_z^{(1)} U^{(5)} [-\eta] \sigma_z^{(5)} U^{(5)\dagger} [\eta] |\psi\rangle_{C(\mathbf{NOT})} = (-1)^{s_2+s_4} |\psi\rangle_{C(\mathbf{NOT})} \quad (\text{A.12})$$

By choosing $\eta = \pi$, these equations give a NOT-gate. This method can be broadened to perform quantum gates on a large-scale cluster state system. Similar to the work of Leung[24], quantum computation can be achieved in cluster states depending on choice of measurement patterns.

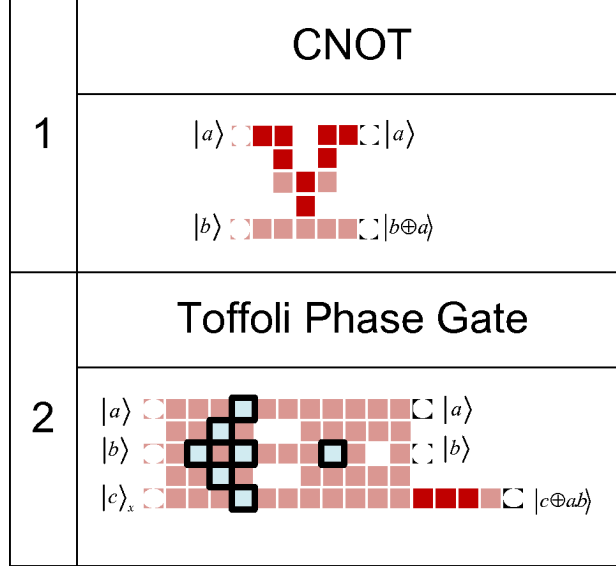


Fig. A.2. Quantum gates in Measurement-Based Quantum Computation. Due to the relationship between CCNOT and Toffoli Phase Gate (TPG), $\text{CCNOT} = H_t(\text{TPG})H_t^\dagger$, the target qubit can be chosen arbitrarily by putting a Hadamard gate on the chosen qubit.

Generally, every quantum gate contains C_l lattice qubits with m measurements, C_w width, and C_h height. In this paper, we will use Raussendorf et al. quantum gates model[4]. As shown in Figure A.2 and Figure A.3, CNOT and Toffoli Phase gate can be performed using measurement on 15 and 54 cluster qubits, respectively.

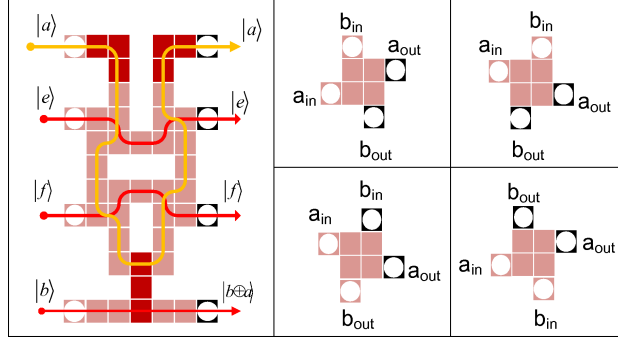


Fig. A.3. Non-adjacent computation. The implementation of four type SWAP gates to propagate the information up-to-down of non-adjacent qubits for performing CNOT. Qubit $|a\rangle$ acts as the control qubit and $|b\rangle$ is the target qubit.

Appendix B Out-of-place and In-place Procedures for Abstract Quantum Carry-Lookahead Adder

Here we summarize the QCLA circuits as proposed by Draper et al.[15]. The circuit for out-of-place addition as shown in Figure B.1 has the form:

1. For $0 \leq i < n$, $Z[i+1] \oplus = A[i]B[i]$ setting $Z[i+1] = g[i, i+1]$.
2. For $0 \leq i < n$, $B[i] \oplus = A[i]$ setting $B[i] = p[i, i+1]$ for $i > 0$ needed to run out-of-place addition circuit.
3. Run the circuit of the P,G, and C networks. Upon completion, $Z[i] = c_i$ for ≥ 1 .
4. For $1 \leq i < n$, $Z[i] \oplus = B[i]$. Now for $i > 0$, $Z[i] = a_i \oplus b_i \oplus c_i = s_i$. For $i = 0$, $Z[i] = b_i$.
5. Set $Z[0] \oplus = A[0]$. For $1 \leq i < n$, $B[i] \oplus = A[i]$. This fixes $Z[0]$, and resets B to initial value.

The addition circuit for in-place operation has form:

1. For $0 \leq i < n$, $Z[i+1] \oplus = A[i]B[i]$ setting $Z[i+1] = g[i, i+1]$.
2. For $0 \leq i < n$, $B[i] \oplus = A[i]$ setting $B[i] = p[i, i+1]$ for $i > 0$ and $B[0] = s_0$.
3. Run the circuit of P,G, and C networks sequences. Upon completion, $Z[i] = c_i$ for ≥ 1 .
4. For $1 \leq i < n$, $B[i] \oplus = Z[i]$. Now $B[i] = s_i$.
5. For $0 \leq i < n-1$, $\neg B$ contains s' .
6. For $1 \leq i < n-1$, $B[i] \oplus = A[i]$.
7. Run the P, G, and network in reverse then upon completion, $Z[i+1] = a_i s'_i$ for $0 \leq i < n-1$, and $B = a_i \oplus s'_i$ for $1 \leq i < n$.
8. For $1 \leq i < n-1$, $B[i] \oplus = A[i]$.

9. $0 \leq i < n-1, Z[i+1] \oplus = A[i]B[i].$

10. $0 \leq i < n-1, \neg B.$

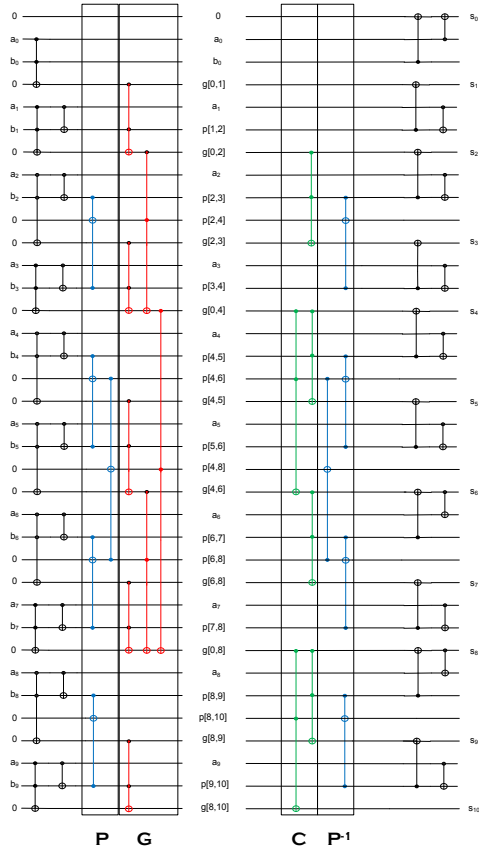


Fig. B.1. Abstract out-of-place Quantum Carry-Lookahead Adder for $n=10$. The blue lines are the Propagate and Inverse Propagate networks; the red line is the Generate network and the green line is the Carry network. The low $n-1$ bits of the carry string are not yet erased .

The resources for each quantum gates in abstract in-place QCLA circuit is provided in the below table:

Table B.1. Logic Gates Resources in Abstract In-Place QCLA

Quantum Gate	Resource
NOT	$2n-2$
CNOT	$4n-5$
TPG	$10n-3w(n)-3w(n-1)-3\lfloor \log_2(n) \rfloor - 3\lfloor \log_2(n-1) \rfloor - 7$

Appendix C Requirements and Performance for Out-of-place and In-place MBQ-CLA

Table C.1. Requirements and Performance of the out-of-place MBQCLA

Parameter	Value
Pitch	4
Variables (Logical Qubits)	$\mathcal{V}(n) = 4n - \lfloor \log_2 n \rfloor + 1$
Width	$Width(n) = 15 \times (\lfloor \log_2(n) \rfloor + \lfloor \log_2(n/3) \rfloor) + 85$
Height	$Height(n) = 4 \times (4n - w(n) - \lfloor \log_2 n \rfloor + 1) - 3$
Area	$Height(n) \times Width(n) =$ $(4 \times (4n - w(n) - \lfloor \log_2 n \rfloor + 1) - 3) \times$ $(15 \times (\lfloor \log_2(n) \rfloor + \lfloor \log_2(n/3) \rfloor) + 85)$
Number of Clustering Operations	$(4n - w(n) - \lfloor \log_2 n \rfloor + 1) \times$ $(15 \times \lfloor \log_2(n) \rfloor + \lfloor \log_2(n/3) \rfloor + 85) - 1) +$ $(15 \times \lfloor \log_2(n) \rfloor + \lfloor \log_2(n/3) \rfloor + 85) \times$ $(4n - w(n) - \lfloor \log_2 n \rfloor)$
Circuit Depth	$\lfloor \log_2(n) \rfloor + \lfloor \log_2(n/3) \rfloor + 7$
Size (Number of Qubits)	$-3271 + 899n - 419w(n) - 377 \lfloor \log_2(n) \rfloor + 56n \lfloor \log_2(2n/3) \rfloor - 14w(n) \lfloor \log_2(2n/3) \rfloor$ $+ 42n \lfloor \log_2(n) \rfloor + 168n \lfloor \log_2(n) \rfloor - 14 \lfloor \log_2(2n/3) \rfloor \lfloor \log_2(n) \rfloor - 42 \lfloor \log_2(n) \rfloor^2$ $+ 6 \times (2n + \sum_{t_p=1}^{\log_2 n - 1} 2(n - 2^{t_p}) + \sum_{t_g=1}^{\log_2 n} 2(2(\lfloor \log_2(n) \rfloor) + (2^{t_g})(\lfloor \log_2 t_g \rfloor))$ $+ \sum_{t_c=1}^{\lfloor \log_2 \frac{2n}{3} \rfloor} 2(n - \lfloor \log_2 t_c \rfloor))$

Table C.2. Requirements and Performance of the in-place MBQCLA

Parameter	Value
Pitch	4
Variables (Logical Qubits)	$\mathcal{V}(n) = 4n - \lfloor \log_2 n \rfloor + 1$
Width	$Width(n) = 15 \times (\lfloor \log_2 n \rfloor + \lfloor \log_2(n-1) \rfloor + \lfloor \log_2 \frac{n}{3} \rfloor + \lfloor \log_2 \frac{n-1}{3} \rfloor) + 157$
Height	$Height(n) = 4 \times (4n - w(n) - \lfloor \log_2 n \rfloor + 1) - 3$
Area	$Height(n) \times Width(n) =$ $(4 \times (4n - w(n) - \lfloor \log_2 n \rfloor + 1) - 3) \times$ $14 \times (\lfloor \log_2 n \rfloor + \lfloor \log_2(n-1) \rfloor + \lfloor \log_2 \frac{n}{3} \rfloor + \lfloor \log_2 \frac{n-1}{3} \rfloor) + 157$
Number of Clustering Operations	$(4n - w(n) - \lfloor \log_2 n \rfloor + 1) \times$ $(15 \times (\lfloor \log_2 n \rfloor + \lfloor \log_2(n-1) \rfloor + \lfloor \log_2 \frac{n}{3} \rfloor + \lfloor \log_2 \frac{n-1}{3} \rfloor) + 156) +$ $(15 \times (\lfloor \log_2 n \rfloor + \lfloor \log_2(n-1) \rfloor + \lfloor \log_2 \frac{n}{3} \rfloor + \lfloor \log_2 \frac{n-1}{3} \rfloor) + 157) \times$ $(4n - w(n) - \lfloor \log_2 n \rfloor)$
Circuit Depth	$\lfloor \log_2 n \rfloor + \lfloor \log_2(n-1) \rfloor + \lfloor \log_2 \frac{n}{3} \rfloor + \lfloor \log_2 \frac{n-1}{3} \rfloor + 14$
Size (Number of Qubits)	$-3068 + 2896n - 138w(n-1) - 162w(n) + 16 \lfloor \log_2 \frac{n-1}{3} \rfloor$ $+ 64n \lfloor \log_2 \frac{n-1}{3} \rfloor - 146 \lfloor \log_2(n-1) \rfloor$ $+ 64n \lfloor \log_2(n-1) \rfloor + 16 \lfloor \log_2(n/3) \rfloor + 64n \lfloor \log_2(n/3) \rfloor$ $+ 21 \lfloor \log_2(n) \rfloor + 64n \lfloor \log_2(n) \rfloor$ $- 16 \lfloor \log_2(n-1) \rfloor \lfloor \log_2(n) \rfloor - 16 \lfloor \log_2 \frac{n}{3} \rfloor \lfloor \log_2(n) \rfloor - 16 \lfloor \log_2(n) \rfloor^2 +$ $6 \times (4n - 1) + 4 \sum_{t_p=1}^{\log_2 n - 1} 2(n - 2^{t_p}) + 2 \sum_{t_g=1}^{\log_2 n} 2(2(\lfloor \log_2(n) \rfloor) + (2^{t_g})(\lfloor \log_2 t_g \rfloor))$ $+ 2 \sum_{t_c=1}^{\lfloor \log_2 \frac{2n}{3} \rfloor} 2(n - \lfloor \log_2 t_c \rfloor)$